

Attacks and Defenses for Free-Riders in Multi-Discriminator GAN

Zilong Zhao^{*§}, Jiyue Huang^{*§}, Stefanie Roos^{*}, Lydia Y. Chen^{*}

^{*}TU Delft, The Netherlands. {Z.Zhao-8, J.Huang-4, S.Roos, Y.Chen-10}@tudelft.nl

Abstract—Generative Adversarial Networks (GANs) are increasingly adopted by the industry to synthesize realistic images using competing generator and discriminator neural networks. Due to data not being centrally available, Multi-Discriminator (MD)-GANs training framework employ multiple discriminators that have direct access to the real data. Distributedly training a joint GAN model entails the risk of free-riders, i.e., participants that aim to benefit from the common model while only pretending to participate in the training process. In this paper, we conduct the first characterization study of the impact of free-riders on MD-GAN. Based on two production prototypes of MD-GAN, we find that free-riders drastically reduce the ability of MD-GANs to produce images that are indistinguishable from real data, i.e., they increase the FID score — the standard measure to assess quality of generated images. To mitigate the model degradation, we propose a defense strategy against free-riders in MD-GAN, termed DFG. DFG distinguishes free-riders and benign participants through periodic probing and clustering of discriminators’ responses based on a reference response of a free-riders, which then allows the generator to exclude the detected free-riders from the training. Furthermore, we extend our defense, termed DFG+, to enable discriminators to filter out free-riders at the variant of MD-GAN that allows peer exchanges of discriminators networks. Extensive evaluation on various scenarios of free-riders, MD-GAN architecture, and three datasets show that our defenses effectively detect free-riders. With 1 to 5 free-riders, DFG and DFG+ averagely decreases FID by 5.22% to 11.53% for CIFAR10 and 5.79% to 13.22% for CIFAR100 in comparison to an attack without defense. In a shell, the proposed DFG(+) can effectively defend against free-riders without affecting benign clients at a negligible computation overhead.

Index Terms—Multi-Discriminator GANs, Free-rider attack, Defense

I. INTRODUCTION

Generative Adversarial Networks (GANs) are an emerging methodology to generate synthetic data [2], [10], [28], [39], especially for the visual data. GANs are capable of generating real-world-like images and are increasingly adopted by the industry for data augmentation and refinement [26]. They owe their success to their unique architecture of two competing neural networks, called discriminator and generator. Training GANs centrally means training a single generator and discriminator iteratively, where the former generates realistic images to fool the discriminator, and the latter then gives feedback to the generator by comparing the generated and real images. As a consequence of privacy regulations imposed on data sources, e.g., GDPR [32] and HIPAA [3], GANs often have to employ

distributed architectures such that they can learn from multiple sources without illegally sharing the raw data.

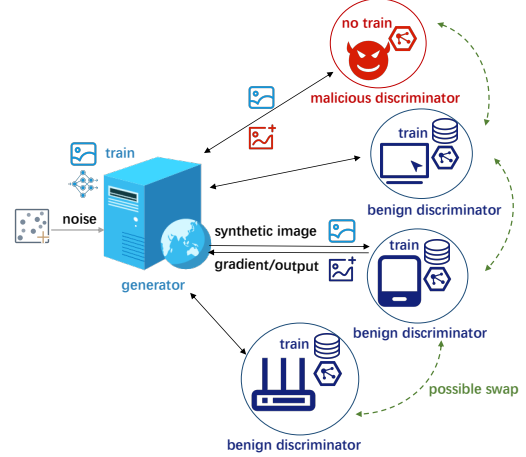


Fig. 1: Architecture of Multi-Discriminator GAN: one generator, and four discriminators, one of which being free-rider.

Multi-Discriminator GAN (MD-GAN), Distributed GAN architecture have been adopted in medical and financial domains [4], [6], [13], [29], [37] that have stringent privacy constraints. Typically, as shown in Fig. 1, there are one generator and multiple discriminators, one discriminator for each data source. To learn such an MD-GAN, an iterative training procedure between generator and discriminators takes place. The generator synthesizes images that imitate the real data, whereas the discriminators provide feedback to the generator based on their local image set. Discriminators can also exchange their local networks with peers in a variant architecture of MD-GAN [13]. Though such a distributed architecture guarantees that raw data is not shared, it increases the chance of misbehaving discriminators, such as free-riders, and increases the difficulty of defending against them.

Free-riders are commonly observed in distributed systems where there are multiple users participate, e.g., peer-to-peer networks [7], [8], [23] or Federated Learning systems [25], [34]. Free-riders in Federated Learning systems [9], [20] try to gain access to the so-called global model from the server, which is aggregated from local models of all contributors without sharing local data. Here, free-riders can simply return the previous global model (possibly with perturbation added) as their contribution. In the context of MD-GAN systems, free-riders aim to gain access to the valuable well-trained generator model without using any real data and providing

[§]Equal contribution

any meaningful feedback to the generator. Different from the Federated Learning system where the model on the server has the identical structure of all of the clients, free-riders in MD-GAN do not have any information about the global view of the generator and other discriminator networks. Moreover, it is no mean feat to defend against free-riders in MD-GAN as the generator only receives the distributed feedback on how well the synthetic images compared to the real ones, i.e., gradients backpropagated from the discriminator.

In this paper, we aim to answer two research questions: what is the impact of free-riders on production prototypes of MD-GAN and how can benign participants defend against such free-riders? Specifically, we consider two MD-GAN variants: (i) MD-GAN^s: discriminators only communicate with the generator [4], [6], [29]). and (ii) MD-GAN^w: discriminators perform model exchanges, in a peer-to-peer way, to avoid over-fitting to their local data [13]. We conduct the first empirical characterization study on how different the number of free-riders affects the quality of synthetic images of MD-GAN when training image benchmarks. Our results show that a small fraction of free-riders in the system can cause degradation of the MD-GAN performance, especially for MD-GAN^w, i.e., synthetic images are highly dissimilar to the real ones, as measured by a high Fréchet Inception Distance (FID) score [15].

Secondly, we propose a novel Defense strategy against the Free-riders on MD-GAN, termed DFG, where generator can filter out the contributions of free-riders. The two key steps of DFG are (i) the generator periodically sends out a probing data set to all discriminators, and (ii) clusters their responses in combination with the reference response of the "detector", a free-rider trained on the generator side. As the variant of MD-GAN considered here allows the discriminators to periodically swap models, we further extend the defense, termed DFG+, and introduce the third defense step at the discriminators. Specifically, the discriminators cluster peers' pair-wise distance vector sent by the generator and avoid exchange updates with free-riders. Consequently, DFG+ can avoid model leakage to discriminators while keeping the training benefits brought by swapping.

We evaluate DFG and DFG+ on different combinations of percentages of free-riders and variants of MD-GAN on MNIST, CIFAR10 and CIFAR-100 data sets. Our results show that DFG(+) can exclude the free-riders with 100% accuracy in both variants of MD-GAN even if half of the nodes in the system are free-riders. When we vary number of free-riders from 1 to 5, DFG and DFG+ averagely decreases FID by 5.22% (MD-GAN^s) and 11.53% (MD-GAN^w) for CIFAR10 and 5.79% (MD-GAN^s) and 13.22% (MD-GAN^w) for CIFAR100 in comparison to an attack without defense.

The main contributions of this paper are two fold. A first kind of characterization of free-riders on two variants of production prototypes of MD-GAN is presented in Section II. We propose a novel and effective defense strategy DFG and its extension DFG+ in section III, and evaluate them on two image benchmarks in Section IV. Our code is temporarily hosted

on google drive¹ with a detailed description for reproducing the results. We plan to provide the source code via Github after publication of the paper.

II. FREE-RIDERS ON MD-GAN

To quantitatively illustrate the impact of free-riders, we first introduce two architecture variants of MD-GAN, which differ in their level of discriminator interaction, and present our free-rider threat model and its impact on MD-GAN.

A. System of MD-GAN prototypes

Key components of MD-GAN are one server and N clients maintaining one generator and N discriminators, respectively. In general, generator and discriminators are all deep neural networks² characterized by their model weights. The generator network, \mathcal{G} , aims to synthesize images that are indistinguishable from real ones. On the other hand, each of the N discriminator networks, $\mathcal{D}_i, i \in \{1, 2, \dots, N\}$, has direct accesses to its own set of real images, X_i . They aim to correctly differentiate fake images generated by generator from real images. Concretely, for an image s , $\mathcal{D}_i(s)$ gives the probability that s is real from the view of the i -th discriminator. Fig. 1 illustrates an example of one generator and four discriminators.

To train an MD-GAN, the generator and discriminators take turns to train and update their network weights over multiple rounds until reaching convergence. Following the structure of WGAN-GP [12], the overall objective is composed of discriminator loss and generator loss functions, where the former captures the real/fake image classification errors and the latter captures the classification mistakes on the generated images. One training round contains multiple mini batches of data. For batch j at round t , \mathcal{G} produces a synthetic dataset $S_{t,i}^j$ from an input vector of Gaussian noise $z_{t,i}^j$ for the i^{th} discriminator.

Discriminator training: The discriminator uses its local real images X_i^j (i.e., real image mini batch j at i^{th} discriminator) and the fake images $S_{t,i}^j$ from the generator to train itself. Specifically, the generator remains fixed during the discriminator training, we only optimize the discriminator loss and updates the weights of discriminator networks through stochastic gradient decent algorithms [31].

Generator training: When calculating generator loss, one can imagine that generator and discriminator are connected as one neural network. The i^{th} discriminator calculates loss for fake images $S_{t,i}^j$ from the generator and back-propagates gradients. During the phase of generator training, weights of the discriminators remain fixed, only generator uses the gradients to update. After \mathcal{G} receives all of the back-propagated gradients of fake images $S_{t,i}^j$ from every i^{th} discriminator, the generator accumulates the gradients from all the discriminators and update its network weights at once.

There are two variant architectures, MD-GAN^s and MD-GAN^w. In addition to iteratively training discriminators and generator networks in every round, MD-GAN^w allows a third

¹<https://drive.google.com/file/d/1QZxpoZpajpFf1LsLTluc151sKPzYbKyF/view?usp=sharing>

²We interchangeably use terms of networks and models

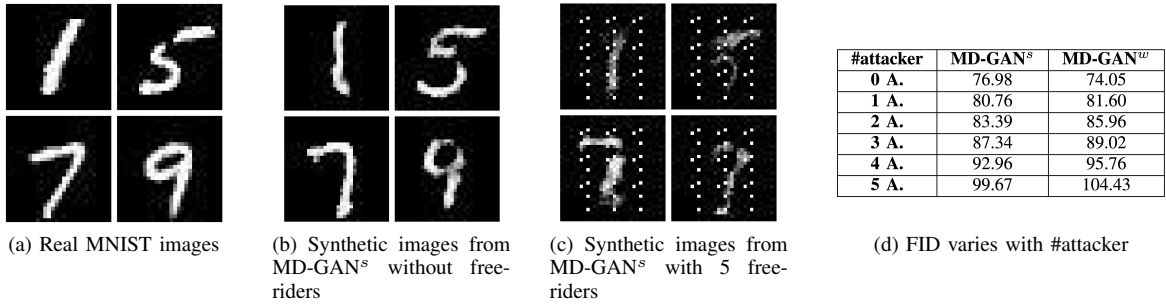


Fig. 2: Real v.s. synthetic MNIST images from generators of MD-GAN encountering 0 and 5 free riders with 5 benign discriminators. The difference of FID scores across different number of free-riders.

step of *swapping discriminators' network weights*. Every E rounds, the generator randomly pairs discriminators to perform a peer-to-peer swapping process, i.e., exchanging their model weights. After swapping, the discriminators replace the previous model with the latest swapped model. Such an architecture intends to avoid over-fitting on local data for each discriminator [13].

Communication model. We assume the communication among the generator and discriminators is reliable and provides in-order delivery, i.e., messages do not get lost or re-ordered. In practice, we use TCP to ensure both properties. For simplicity, all parties are online all the time under our system and provide timely responses in each round. The generator only proceeds to its training after receiving all gradient updates from all discriminators. Note that it is possible to deal with offline clients [29] but modeling such behavior realistically is out of the scope of this paper.

Implementation MD-GAN is implemented using the Pytorch v1.8.1 RPC framework. This choice enables the generator to control the flow of training steps with ease. Clients just join the group, then wait to be initialized and assigned tasks. To parallelize the training across all clients, RPC provides a function `rpc_async()` that allows the generator to make non-blocking RPC calls to run functions at a client. To implement synchronization points, RPC provides a blocking function `wait()` for the return from a previous call to the function `rpc_async()`. The return of `rpc_async()` is a *future* type object. Once the `wait()` is called on this object, the process is blocked until the return values are received from the client. We use `rpc_async()` for both training the generator and discriminators networks. The training of the generator network does not continue until it receives input from all discriminators and vice versa. For MD-GAN^w, the swapping process also blocks the training via `rpc_async()`.

One weakness of the current RPC framework on Pytorch v1.8.1 is that it does not support the transmission of tensor, (i.e., where all the model weights and images are loaded in memory) directly on GPU through an RPC call. This means that each time when we collect or update the model weights, we introduce an extra delay to detach the weights from GPU to CPU or reload the weights from CPU to GPU.

B. Free-rider adversarial model

We consider free-riders on the discriminator side, i.e., clients want to obtain the final generator model without contribution to the training of MD-GAN. Their goal is not to degrade the image quality of the generator but the contrary. In this sense, they are rational parties rather than malicious. They deviate from the expected learning procedure to gain utility, namely access to the generator model.

Such free-riders are local, internal, and active adversaries. In other words, they can only observe and participate in the communication and computation of their own training process. Moreover, free-riders do not own any data for training MD-GAN, nor do they have access to the data of others. They do not collude. The assumption of non-collusion is sensible as additional free-riders might decrease the quality of the final model they obtain, so parties are unlikely to reveal their free-riding to others.

We specifically consider free-rider attacks with respect to MD-GAN architecture variants. As discriminators participate in both the training of the discriminator and generator, free-riders take the following actions accordingly. When training the discriminator, due to lack of local data, free-riders randomly initialize the weights of their discriminator network for both variants of MD-GAN. The weights follows Kaiming initialization [14]. In order to provide the gradients needed in training the generator, free-riders use their randomly initialized discriminators to inference the synthetic images from generator and back-propagate. For MD-GAN^w, if they manage to swap with other discriminators, they return the gradients using the discriminator model they have received from their latest swap; otherwise, the randomly initialized model is used.

C. Impact of free-riders

To show the impact of free-riders on MD-GAN, we empirically evaluate the quality of generated images when experiencing different numbers of free-riders. We compare the generated images with the real ones using FID, the standard measure for the similarity of features between images. The lower the FID value, the better quality the generated images. The FID value is expected to decrease with the training rounds.

We performed the experiments on MNIST, CIFAR10, and CIFAR100. Due to space constraints, we only present the

results for MNIST in this section. We include the result of CIFAR10 and CIFAR100 in Sec. IV when comparing the system with and without defense. We keep the number of benign clients constant at 5 and vary the number of free-riders between 0 and 5. Results are averaged over 3 runs and we train for 100 rounds; with these numbers, a single run of training MD-GAN takes on average around 140 minutes on our prototype. More details about the experimental setup are summarized in Sec. IV-B.

Fig. 2 displays the impact of free-riding through both illustration and concrete values. Fig. 2c and Fig 2b highlight the quality difference between the synthetic images when encountering 0 and 5 free-riders, respectively, for MD-GAN^s. Free-riders clearly degrade the capacity of MD-GAN^s in generating realistic images. This intuition is quantified by the FID in Fig. 2d. Furthermore, when there are no free-riders, MD-GAN^w converges better than MD-GAN^s. That is because swapping prevents discriminators from over-fitting on their local data. With the increasing number of free-riders in the system, the performance of MD-GAN^s and MD-GAN^w degrades. MD-GAN^w deteriorates more than MD-GAN^s for same number of free-riders, because swapping with free-riders destroys all the previous training effort of a benign client. The result illustrates that free-riders, though they do not intend to negatively affect the final result, have a concerning negative impact on performance, emphasizing the need for defenses.

III. DEFENDING MD-GAN AGAINST FREE-RIDERS

After introducing models and goals, we propose DFG(+) (i.e., DFG and DFG+), a defense strategy against free-riders in MD-GAN. The key elements of DFG(+) are a probing generated image set \hat{S} and a detector \mathcal{D}_{N+1} . \mathcal{D}_{N+1} is a free-rider run by the generator to obtain a reference model for free-rider responses. As MD-GAN^w allows discriminators to swap local model weights, we further enhance the defense for the discriminators, termed DFG+. DFG+ provides discriminators with information about the similarity across their responses on the probing set \hat{S} and enables them to strategically accept or reject swaps. Fig. 3 illustrates the steps and the differences in the defenses.

The **objectives of the DFG** are three-fold:

- 1 Accurately detecting free-riders in each round and excluding their gradients from accumulation.
- 2 Improving the FID for the case when free-riders are present but not considerably decreasing the FID in the absence of free-riders.
- 3 Entailing low additional overhead.

Note that the first goal also implies that benign clients should not be classified as free-riders. The second part of the second goal is important as a defense that decreases the performance, e.g., by excluding benign clients, in the absence of an attack is unlikely to be adopted, especially if the impact of a low number of free-riders is less than the decrease in image quality caused by the defense. The last goal is particularly important because the generator and discriminators might be unwilling to deploy a defense that

considerably increases delays, computation, or communication overhead.

We analyze the overhead of the defense theoretically at the end of the section and provide experimental results to confirm that we achieve the first two objectives in Section IV.

A. Protocol of DFG

Step 1: In our defense, \mathcal{G} periodically, i.e., every L rounds, generates a probing set \hat{S} to the clients. The set can act as a replacement for $S_{t,i}^j$ (i.e., synthetic image at round t and batch j of the i^{th} discriminator). In contrast to the standard algorithm, DFG sends the same set \hat{S} to all clients. The clients evaluate their discriminators on the set \hat{S} and return the results in the form of a vector. Concretely, for each image s_k , with $1 \leq k \leq |\hat{S}|$, discriminator \mathcal{D}_i computes $\mathcal{D}_i(s_k)$ and the returned vector is:

$$Pr_i(\hat{S}) = (\mathcal{D}_i(s_1), \mathcal{D}_i(s_2), \dots, \mathcal{D}_i(s_{|\hat{S}|})).$$

Step 2: Additionally, to model how free-riders behave, \mathcal{G} makes use of a detector. The usage of the detector is sharing the same thought as the usage of oracle as a reference in active learning for defending attacks [35], [36], [38]. Concretely, the generator randomly initializes a discriminator \mathcal{D}_{N+1} as a reference model of a free-rider and then computes $Pr_{N+1}(\hat{S})$.

Step 3: After the generator collects all the vectors Pr_i , $1 \leq i \leq N+1$, it applies 2-means clustering based on the distances of the squared L2 norm on all vectors Pr_i . Intuitively, the Pr_i of a benign client is expected to have a low distance to the Pr_i of other benign clients, whereas they have a high distance to the Pr_i of the free-riders, including the detector. Consequently, we classify all clients in the cluster that contains the detector as free-riders.

B. Protocol of DFG+

MD-GAN^w provides both additional challenges and opportunities. A key challenge is that a discriminator is not trained by one single client and hence it is hard to determine whether one party has trained properly. Free-riders can obtain a properly trained discriminator by swapping, and then compute the gradients of images from the generator. This further exacerbate the difficulty of differentiating the gradients obtained from free-riders and benign discriminators. To introduce a discriminator-side defense, we take advantage of one information: the benign discriminators know that they are not free-riders. So once a benign client is asked to swap with another that is suspected to be a free-rider, it can refuse.

DFG+ utilizes this extra information to guide the swapping process by adding three more steps to DFG.

Step 4: After the generator has all the vectors Pr_i , $1 \leq i \leq N+1$, they compute a $(N+1) \times (N+1)$ matrix V of pair-wise L2 distances between the Pr of the discriminators, including the detector, i.e., the element V_{ij} is $\|Pr_i - Pr_j\|_2$. The generator shares the computed distances $V_{i1}, \dots, V_{i(N+1)}$ with the i^{th} client.

Step 5: A benign client i then performs 2-means clustering on these distances, excluding V_{ii} . The cluster with lower mean distances is taken to be the cluster of benign clients. The

underlying assumption here is that the differences between properly trained discriminators is less than between randomly initialized ones.

Step 6: A benign client only swaps with parties that are in the same cluster as it according to its local clustering.

While our protocol cannot dictate the behavior of free-riders (as they may choose not to follow the protocol), in our evaluation, free-riders always accept swap requests as they hope to obtain better models.

C. Overhead

We discuss the computation and communication complexity of DFG and DFG+ in relation to the complexity of MD-GANs without any defense. We start by analyzing the additional computation overhead, which is the main cost factor as by our experiments.

Computation DFG: In DFG, note that the clients need to compute $D_i(s_k)$ for $s_k \in \hat{S}$. However, when training without the defense, they also need to compute $D_i(s'_k)$ for $s'_k \in S_{t,i}^j$ with $|S_{t,i}^j| = |\hat{S}|$ to evaluate the quality of their current model. Hence, there is no additional overhead on the client-side with regard to computation. The generator has to compute the pair-wise distances between $N + 1$ vectors of length $|\hat{S}|$ and perform a 2-means clustering of $N + 1$ values. The distance computation has complexity $\mathcal{O}(|\hat{S}|N^2)$ and the k-means clustering has complexity $\mathcal{O}(N^2)$. As the number of images is expected to be much larger than the number of clients, we have a complexity of $\mathcal{O}(|\hat{S}|N^2)$. In comparison, the cost of a training round without DFG is $\mathcal{O}(|\hat{S}|MQ)$ where M is the image size and Q a factor related to the structure and size of the neural network [24]. According to the real world application of MD-GAN [4], M should be much larger than N^2 , meaning that the computation complexity of the normal MD-GAN execution by far exceeds the complexity of DFG.

Computation DFG+: For DFG+, the clustering is also performed on the client-side, incurring an overhead of $\mathcal{O}(N^2)$ for each client. As for DFG, the training complexity exceeds the complexity of DFG+ by far.

Communication DFG: The only additional communication overhead is on the client-side, namely sending the values $D_i(s_k)$ to the generator. Hence the communication complexity is $\mathcal{O}(N|\hat{S}|)$. During a normal MD-GAN round, the generator sends $N|\hat{S}|$ images of size M , so the complexity is $\mathcal{O}(MN|\hat{S}|)$, much higher than for DFG.

Communication DFG+: For DFG+, the generator sends N vectors of length $N + 1$ that allow the clients to perform clustering, so the communication complexity of DFG+ is $\mathcal{O}(N|\hat{S}| + N^2)$. In practice, we expect a low number of clients in comparison to images, so $\mathcal{O}(N|\hat{S}|)$ is the dominating factor, which, as explained for DFG, is much lower than the complexity of an MD-GAN execution without defense.

Overall, the complexities of DFG and DFG+ are much lower than those of the standard training, so that they do not add overheads that might discourage use of the defenses.

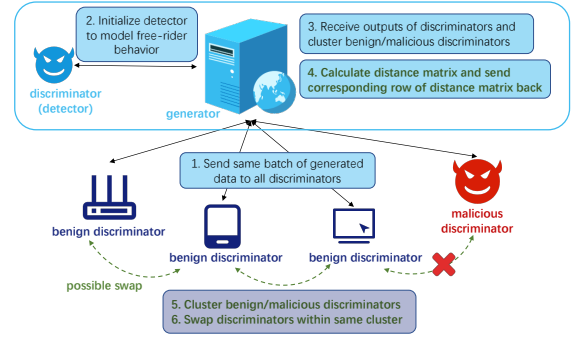


Fig. 3: Key steps of DFG(+): step 1-3 are common to MD-GAN^s and MD-GAN^w, whereas step 4-6 are specific to MD-GAN^w only.

IV. EXPERIMENTAL EVALUATION

Our defense DFG and DFG+ are evaluated on three widely used image datasets, and compared with the scenarios without defense. To evaluate the efficiency of DFG, we resort to the precision and recall of the identified free-riders. And for DFG+, we also report how many malicious swap requests our defense prevents. We furthermore conduct an experiment without the detector to show-case its importance to correctly identify free-riders.

A. Evaluation Metrics

To evaluate all the experiments, we test the final performance of \mathcal{G} . Since our use case is image classification, we choose to use Fréchet inception distance (FID) [15] defined as follows:

$$\text{FID} = \|\mu_1 - \mu_2\|^2 + \text{tr}(\Sigma_1 + \Sigma_2 - 2(\Sigma_1 \Sigma_2)^{1/2})$$

where μ_1 and μ_2 denote the feature-wise mean of the real and generated images, Σ_1 and Σ_2 refer to the covariance matrix for the real and generated feature vectors. $\|\mu_1 - \mu_2\|^2$ refers to the sum squared difference between the two mean vectors, and tr is the trace linear algebra operation. Intuitively, the lower the FID, the closer the generated and real images.

To show the efficiency of DFG and DFG+, we use two different metrics. For DFG, the **precision** and **recall** of the identified "free-riders" are reported. The precision quantifies the fraction of predicted "free-riders" are actual real free-riders. The recall is to measure the fraction of true free-riders identified by our defense. Free-rider and benign client are labelled as Positive and Negative for the calculation [27]. Note that recall is not defined in the absence of free-riders.

For DFG+, our focus lies in preventing discriminator swapping between benign and malicious clients. If benign clients swap with benign clients or malicious clients swap with malicious clients, we regard it as correct action. But if the DFG+ prevents a swapping request between two benign clients, we see this as a **wrong prevention**. And if DFG+ does not stop a swapping between a benign and a malicious client, we call this a **wrong permission**. We count all the actions above and report their relative frequency.

B. Experimental setup

Datasets. We test our algorithms on three commonly used image datasets: MNIST [17], CIFAR10 [16] and CIFAR100 [16]. MNIST contains 60 000 grayscale (10 classes) while CIFAR10 and CIFAR100 have 50 000 colorful (10/100 classes) training images. Each benign client possesses 5 000 images, which are evenly distributed over all of the classes.

Baselines. To show the efficiency of DFG and DFG+, we run the algorithms MD-GAN^s and MD-GAN^w with (i.e., **DFG_Simple** and **DFG+_Swap**) and without (i.e., **No_Def_Simple** and **No_Def_Swap**) defense. We fix the number of **benign clients to 5** for all experiments and vary the number of malicious clients (i.e., free-riders) from 0 to 5. The total number of training rounds is 100. \mathcal{G} generates 10 000 images every 5 rounds and they are used to evaluate \mathcal{G} 's performance in terms of FID. Every 10 rounds, we execute DFG and DFG+: the generator sends the same probing set \hat{S} of 500 images to all clients and the detector, though \hat{S} varies over rounds.

For all experiments, we choose to use Wasserstein GAN with Gradient Penalty (WGAN-GP) [12] structure as generator and discriminator models. The network of each discriminator consists of three repeated blocks. Each block concatenates 2D Convolution, Instance Normalization and Leaky Relu layers. \mathcal{G} is also composed of three concatenating blocks. Each block contains 2D Transposed Convolution, Batch Normalization and Relu layers. The batch size B is set to 500. Since each client owns 5 000 images, there are 10 mini batches per training round. Due to the characteristics of WGAN-GP, the generator is trained once for every 5 times the discriminators are trained. Therefore, for each round, the discriminator is trained 10 times by all mini batches, but the generator is only trained twice. For DFG and DFG+, when they evaluate the quality of discriminator every 10 rounds, they only do that during the first training batch out of two within the round. We repeat each experiment 3 times and report the average.

Testbed. Experiments are run on two machines, both running Ubuntu 20.04. Each machine is equipped with 32 GB memory, GeForce RTX 2080 Ti GPU and 10-core Intel i9 CPU. Each CPU core has two threads, hence each machine contains 20 logical CPU cores in total. One machine hosts the generator, the other hosts all the discriminators. The machines are interconnected via 1G Ethernet links.

C. Results

1) *DFG and DFG+ for MD-GAN^s and MD-GAN^w*: Tab. I shows the final FID of MD-GAN^s and MD-GAN^w with and without defenses (i.e., DFG and DFG+). DFG and DFG+ improve the final performance of the generator. The DFG+ improvement for MD-GAN^w is higher than the improvement made by DFG for MD-GAN^s. That is because, as detailed in Section II, the impact of the attack is greater on MD-GAN^w, so there is more room for improvement. With 1 to 5 free-riders, DFG and DFG+ averagely decrease FID by 5.22% (MD-GAN^s) and 11.53% (MD-GAN^w) for CIFAR10 in comparison to an attack without defense. For CIFAR100, the decrease is

even slightly higher, namely 5.79% (MD-GAN^s) and 13.22% (MD-GAN^w).

For all the experiments on CIFAR10 and CIFAR100, the precision and recall of the recognition of free-riders by DFG are **100%**. That means for the experiments with free-riders, DFG correctly identifies all the attackers. And for the experiments without free-riders, DFG never wrongly excludes any benign client. For DFG+, the ratio of correct preventions and permissions is also **100%** for all the experiments. It signifies that all the swaps are between two benign clients or two free-riders, but never between a free-rider and a benign client. Thus, Objective 1 from Section III, i.e., correctly identifying free-riders, is achieved. There are no bold results for 0 attacker in Tab. I because there is no statistically significant difference between having a defense and not having a defense. This result shows that our defense does not negatively impact FID, thus fulfilling Objective 2 from Section III.

The improvement from the defenses is more pronounced when the number of attackers is high. With an increasing number of free-riders, the harm accumulates in the system. But with our defenses, all the free-riders are correctly identified and excluded. The only damage for the system comes from the first 10 rounds before our defenses are applied.

2) *Ablation study*: To show the efficacy of the detector, we propose an ablation experiment without the detector. Therefore, we adjust DFG to DFG_A: after step 3 in Fig. 3, DFG_A calculates the pairwise distances of the N clients without the detector and then calculates the sum of distances for each discriminator. To determine free-riders, DFG_A uses 2-means to cluster the sum of distances. The group with the higher mean is treated as the cluster of free-riders. The motivation behind this design is based on the conjecture that outputs from benign clients should be similar and far from free-riders. For adapted DFG_A+, the only difference to DFG+ is that there is no distance to the detector in the vector provided to the clients. Due to the page limit, we only present the experiments with 0 and 5 attackers. The setup is the same as in Sec. IV-B.

Tab. II and Tab. III compare DFG_A and DFG_A+ with DFG and DFG+ for both MD-GAN^s and MD-GAN^w. The values in Tab. II and Tab. III are the absolute difference of the various metrics between DFG/DFG_A and DFG+/DFG_A+, respectively. For instance, the value -12.77% in the third row and second column of Tab. II indicates that the FID of DFG is 12.77% lower — and hence better — than the one of DFG_A. DFG_A and DFG_A+ wrongly exclude benign clients if there is no attacker. This degradation in the absence of attacks happens because the clustering always divides the clients in two clusters, with one of them being treated as free-riders. In the absence of actual free-riders, benign clients are excluded. DFG_A also excludes benign clients for the case of 5 attackers, indeed it is more likely to exclude benign clients than free-riders. DFG_A+ fares slightly better for the case of 5 attackers but still misclassifies some benign clients as free-riders and vice versa. The misclassification happens when the distances between different free-riders are similar to

TABLE I: Final FID for MD-GAN^s and MD-GAN^w (A. is short for free-rider attacker).

Method	CIFAR100						CIFAR10					
	0 A.	1 A.	2 A.	3 A.	4 A.	5 A.	0 A.	1 A.	2 A.	3 A.	4 A.	5 A.
No_Def_Simple	80.45	85.54	86.14	87.62	92.34	96.07	78.59	81.71	84.86	86.06	92.01	95.67
DFG_Simple	80.98	81.36	82.98	85.01	86.43	88.21	78.15	80.32	81.25	82.34	84.15	85.96
No_Def_Swap	79.40	89.83	92.51	95.52	99.28	101.37	78.36	90.36	92.55	95.70	98.09	101.98
DFG+_Swap	79.35	79.69	82.94	84.62	85.69	90.31	78.83	80.31	81.45	81.89	85.46	86.01

those between benign clients, so that the generator assumes the wrong cluster to consist of free-riders. The experiment illustrates the need for a detector as a reference point.

TABLE II: Positive impact of detector for DFG on MD-GAN^s

Metrics	CIFAR100		CIFAR10	
	0 A.	5 A.	0 A.	5 A.
FID	-12.77%	-10.44%	-13.81%	-15.41%
Precision	+100%	+51.18%	+100%	+79.20%
Recall	-	+73.34%	-	+88.89%

TABLE III: Positive impact of detector for DFG+ on MD-GAN^w

Metrics	CIFAR100		CIFAR10	
	0 A.	5 A.	0 A.	5 A.
FID	- 7.07%	- 8.58%	- 20.58%	-7.79%
Precision	+100%	+44.83%	+100%	+75.54%
Recall	-	+64.45%	-	+47.62%
Correct Prev. & Perm.	0%	0%	0%	0%
Wrong Prevention	-48.15%	0%	-88.89%	0%
Wrong Permission	0%	0%	0%	0%

V. RELATED WORK

In this section, we summarize the related studies on multi-discriminator GAN frameworks [4], [6], [13], [29] and free-riders attacks in distributed learning systems [9], [20].

MD-GAN: Overcoming the data privacy issues of centralized GANs [18], [19], [21], distributed GANs [4], [6], [11], [13], [29], [30] enable multiple data owners to collaboratively train GAN systems. Existing distributed GAN frameworks can be summarized as Federated Learning GANs (FLGANs) [11], [30] and MD-GANs [4], [6], [13], [29]. In FLGANs, a client trains both a generator and a discriminator network and a server aggregates both networks from all clients. Specifically, FedGAN [30] addresses the issue of heterogeneous data sources subject to communication and privacy constraints and provides a convergence guarantee. FeGAN [11] then focuses on the system view to overcome mode collapse and learning divergence problems arising from a distributed setup. Its main contributions are Kullback-Leibler (KL) weighting and a balanced sampling scheme. Training an entire GAN is computation intensive, especially for the generator. Thus, the implicit prerequisite for FLGANs is that clients have sufficient computational capacity. In contrast, MD-GAN architectures offload the intensive training of the generator to the server and keep the lighter training of the discriminator on the client side. In this manner, MD-GANs are also able to involve a massive number of edge nodes [5], [33]. The various architectures of MD-GAN differ with regard to model exchange between discriminators. AsynDGAN [4] and GMAN [6] are elementary

MD-GAN architectures where discriminators only directly communicate with the generator. In order to improve the drawbacks of MD-GAN when discriminators only own small datasets, Hardy et al. [13] propose that discriminators are swapped between clients, opening an opportunity for free-riders to act stealthily.

Free-riders: The concept of free-riders first emerged in economics [1] but has been essential in various of distributed systems. In peer-to-peer file-sharing systems, free-riders join to download files without uploading any files [7], [22]. In Federated Learning systems [25], [34], Lin et. al. [20] first propose stealthy free-rider attacks for image classification: instead of sending a random model, free-riders send the global model of the previous round back with small perturbation noises added or provide a fake gradient using the previous difference of weights. Defenses are designed accordingly based on the DAGMM [40] network, which is a recent anomaly detection method so as to catch the differences on deep feature by gradients for free-riders. Fraboni et. al. [9] further explore the attack of adding perturbation noises of [20] to provide convergence guarantee of the global model in the presence of a single free-rider. This work establishes the theoretical support for global convergence using a similar attacking strategy. However, as both studies are concerned with Federated Learning systems, where the clients and the server are curating models of the same structure, they are not directly applicable to MD-GAN systems where the server and client train different types of models. Additionally, none of them has provided a systematic study on the influence of (multiple) free-riders. To the best of our knowledge this paper is the first to study free-riders in MD-GANs.

VI. CONCLUSION

In this paper, we first showed that MD-GANs suffer noticeably from free-rider attacks, especially for MD-GAN^w where the discriminators exchange local models. With 1 to 5 free-riders, our defense, DFG(+), averagely increases the quality of the synthetic images by 5.22% (MD-GAN^s) and 11.53% (MD-GAN^w) for CIFAR10 and 5.79% (MD-GAN^s) and 13.22% (MD-GAN^w) for CIFAR100.

In our experiments, the defenses are always successful in classifying free-riders and benign nodes when a detector is present. However, while all free-riders initialize different random models, they all use the same methodology for initialization as the detector. If that is not the case, e.g., when free-riders are aware of the defense based on the detector, free-riders are still expected to perform very differently than benign nodes and hence we do not expect them to be misclassified.

It is future work to verify this expectation and ensure that defenses can mitigate free-riders if these free-riders are aware of the defense.

REFERENCES

- [1] W. J. Baumol. Welfare economics and the theory of the state. In *The encyclopedia of public choice*, pages 937–940. Springer, 2004.
- [2] A. Brock, J. Donahue, and K. Simonyan. Large scale GAN training for high fidelity natural image synthesis. In *7th International Conference on Learning Representations, ICLR 2019, New Orleans, LA, USA, May 6-9, 2019*. OpenReview.net, 2019.
- [3] Centers for Medicare & Medicaid Services. The Health Insurance Portability and Accountability Act of 1996 (HIPAA). Online at <http://www.cms.hhs.gov/hipaa/>, 1996.
- [4] Q. Chang, H. Qu, Y. Zhang, M. R. Sabuncu, C. Chen, T. Zhang, and D. N. Metaxas. Synthetic learning: Learn from distributed asynchronized discriminator GAN without sharing medical image data. In *2020 IEEE/CVF Conference on Computer Vision and Pattern Recognition*, pages 13853–13863, 2020.
- [5] C. Correia, M. Correia, and L. Rodrigues. Omega: a secure event ordering service for the edge. In *50th Annual IEEE/IFIP International Conference on Dependable Systems and Networks, DSN 2020, Valencia, Spain, June 29 - July 2, 2020*, pages 489–501. IEEE, 2020.
- [6] I. P. Durugkar, I. Gemp, and S. Mahadevan. Generative multi-adversarial networks. *CoRR*, abs/1611.01673, 2016.
- [7] M. Feldman and J. Chuang. Overcoming free-riding behavior in peer-to-peer systems. *SIGecom Exch.*, 5(4):41–50, 2005.
- [8] M. Feldman, C. H. Papadimitriou, J. Chuang, and I. Stoica. Free-riding and whitewashing in peer-to-peer systems. *IEEE J. Sel. Areas Commun.*, 24(5):1010–1019, 2006.
- [9] Y. Fraboni, R. Vidal, and M. Lorenzi. Free-rider attacks on model aggregation in federated learning. In A. Banerjee and K. Fukumizu, editors, *The 24th International Conference on Artificial Intelligence and Statistics*, volume 130 of *Proceedings of Machine Learning Research*, pages 1846–1854, 2021.
- [10] Y. Gao, R. Singh, and B. Raj. Voice impersonation using generative adversarial networks. In *2018 IEEE International Conference on Acoustics, Speech and Signal Processing, ICASSP 2018, Calgary, AB, Canada, April 15-20, 2018*, pages 2506–2510. IEEE, 2018.
- [11] R. Guerraoui, A. Guirguis, A. Kermarrec, and E. L. Merrer. Fegan: Scaling distributed gans. In D. D. Silva and R. Kapitza, editors, *Middleware '20: 21st International Middleware Conference, Delft, The Netherlands, December 7-11, 2020*, pages 193–206. ACM, 2020.
- [12] I. Gulrajani, F. Ahmed, M. Arjovsky, V. Dumoulin, and A. Courville. Improved training of wasserstein gans. *arXiv preprint arXiv:1704.00028*, 2017.
- [13] C. Hardy, E. L. Merrer, and B. Sericola. MD-GAN: multi-discriminator generative adversarial networks for distributed datasets. In *2019 IEEE International Parallel and Distributed Processing Symposium, IPDPS 2019, Rio de Janeiro, Brazil, May 20-24, 2019*, pages 866–877. IEEE, 2019.
- [14] K. He, X. Zhang, S. Ren, and J. Sun. Delving deep into rectifiers: Surpassing human-level performance on imagenet classification. In *Proceedings of the IEEE international conference on computer vision*, pages 1026–1034, 2015.
- [15] M. Heusel, H. Ramsauer, T. Unterthiner, B. Nessler, and S. Hochreiter. Gans trained by a two time-scale update rule converge to a local nash equilibrium. In I. Guyon, U. V. Luxburg, S. Bengio, H. Wallach, R. Fergus, S. Vishwanathan, and R. Garnett, editors, *Advances in Neural Information Processing Systems*, volume 30. Curran Associates, Inc., 2017.
- [16] A. Krizhevsky, G. Hinton, et al. Learning multiple layers of features from tiny images. 2009.
- [17] Y. LeCun, L. Bottou, Y. Bengio, and P. Haffner. Gradient-based learning applied to document recognition. *Proceedings of the IEEE*, 86(11):2278–2324, 1998.
- [18] C. Li, D. Alvarez-Melis, K. Xu, S. Jegelka, and S. Sra. Distributional adversarial networks. In *6th International Conference on Learning Representations, ICLR 2018, Vancouver, BC, Canada, April 30 - May 3, 2018, Workshop Track Proceedings*. OpenReview.net, 2018.
- [19] X. Liang, Z. Hu, H. Zhang, C. Gan, and E. P. Xing. Recurrent topic-transition GAN for visual paragraph generation. In *IEEE International Conference on Computer Vision, ICCV 2017, Venice, Italy, October 22-29, 2017*, pages 3382–3391. IEEE Computer Society, 2017.
- [20] J. Lin, M. Du, and J. Liu. Free-riders in federated learning: Attacks and defenses. *CoRR*, abs/1911.12560, 2019.
- [21] G. Liu, I. Khalil, and A. Khreishah. Zk-gandef: A GAN based zero knowledge adversarial training defense for neural networks. In *49th Annual IEEE/IFIP International Conference on Dependable Systems and Networks, DSN 2019, Portland, OR, USA, June 24-27, 2019*, pages 64–75. IEEE, 2019.
- [22] T. Locher, P. Moor, S. Schmid, and R. Wattenhofer. Free riding in bittorrent is cheap. In *5th ACM Workshop on Hot Topics in Networks - HotNets-V*, 2006.
- [23] T. Locher, P. Moore, S. Schmid, and R. Wattenhofer. Free riding in bittorrent is cheap. In *5th Workshop on Hot Topics in Networks (HotNets)*, 2006.
- [24] P. Maji and R. Mullins. On the reduction of computational complexity of deep convolutional neural networks. *Entropy*, 20(4), 2018.
- [25] B. McMahan, E. Moore, D. Ramage, S. Hampson, and B. A. y Arcas. Communication-efficient learning of deep networks from decentralized data. In *AISTATS*, volume 54 of *Proceedings of Machine Learning Research*, pages 1273–1282. PMLR, 2017.
- [26] R. S. Peres, M. Azevedo, S. O. Araújo, M. Guedes, F. Miranda, and J. Barata. Generative adversarial networks for data augmentation in structural adhesive inspection. *Applied Sciences*, 11(7):3086, 2021.
- [27] D. M. W. Powers. Evaluation: from precision, recall and f-measure to roc, informedness, markedness and correlation. *CoRR*, abs/2010.16061, 2020.
- [28] B. Proven-Bessel, Z. Zhao, and L. Chen. Comicgan: Text-to-comic generative adversarial network. *arXiv preprint arXiv:2109.09120*, 2021.
- [29] H. Qu, Y. Zhang, Q. Chang, Z. Yan, C. Chen, and D. N. Metaxas. Learn distributed GAN with temporary discriminators. In *Computer Vision - ECCV 2020 - 16th European Conference, Glasgow, volume 12372 of Lecture Notes in Computer Science*, pages 175–192, 2020.
- [30] M. Rasouli, T. Sun, and R. Rajagopal. Fedgan: Federated generative adversarial networks for distributed data. *CoRR*, abs/2006.07228, 2020.
- [31] H. Robbins and S. Monro. A stochastic approximation method. *The annals of mathematical statistics*, pages 400–407, 1951.
- [32] E. Union. Regulation (eu) 2016/679 of the european parliament and of the council of 27 april 2016 on the protection of natural persons with regard to the processing of personal data and on the free movement of such data, and repealing directive 95/46/ec (general data protection regulation). *Official Journal L110*, 59:1–88, 2016-05-04.
- [33] Z. Wang, H. Xu, J. Liu, H. Huang, C. Qiao, and Y. Zhao. Resource-efficient federated learning with hierarchical aggregation in edge computing. In *40th IEEE Conference on Computer Communications, INFOCOM 2021, Vancouver, BC, Canada, May 10-13, 2021*, pages 1–10. IEEE, 2021.
- [34] Q. Yang, Y. Liu, T. Chen, and Y. Tong. Federated machine learning: Concept and applications. *ACM Trans. Intell. Syst. Technol.*, 10(2):12:1–12:19, 2019.
- [35] T. Younesian, Z. Zhao, A. Ghiassi, R. Birke, and L. Y. Chen. Qactor: Active learning on noisy labels. In *Asian Conference on Machine Learning*, pages 548–563. PMLR, 2021.
- [36] Z. Zhao, R. Birke, R. Han, B. Robu, S. Bouchenak, S. B. Mokhtar, and L. Y. Chen. Enhancing robustness of on-line learning models on highly noisy data. *IEEE Transactions on Dependable and Secure Computing*, 18(5):2177–2192, 2021.
- [37] Z. Zhao, R. Birke, A. Kunar, and L. Y. Chen. Fed-tgan: Federated learning framework for synthesizing tabular data. *arXiv preprint arXiv:2108.07927*, 2021.
- [38] Z. Zhao, S. Cerf, R. Birke, B. Robu, S. Bouchenak, S. B. Mokhtar, and L. Y. Chen. Robust anomaly detection on unreliable data. In *49th Annual IEEE/IFIP International Conference on Dependable Systems and Networks*, pages 630–637, 2019.
- [39] Z. Zhao, A. Kunar, H. V. der Scheer, R. Birke, and L. Y. Chen. CTAB-GAN: effective table data synthesizing. *CoRR*, abs/2102.08369, 2021.
- [40] B. Zong, Q. Song, M. R. Min, W. Cheng, C. Lumezanu, D. Cho, and H. Chen. Deep autoencoding gaussian mixture model for unsupervised anomaly detection. In *6th International Conference on Learning Representations*, 2018.